DOI: 10.1002/adfm.200500792

Mimicking Biological Phenol Reaction Cascades to Confer Mechanical Function**

By *Li-Qun Wu*, *Martin K. McDermott*, *Chao Zhu*, *Reza Ghodssi*, and *Gregory F. Payne**

Phenol reaction cascades are commonly used in nature to create crosslinked materials that perform mechanical functions. These processes are mimicked by electrochemically initiating a reaction cascade to examine if the mechanical properties of a biopolymer film can be predictably altered. Specifically, thin films (≈30–45 μm) of the polysaccharide chitosan are cast onto gold-coated silicon wafers, the chitosan-coated wafers are immersed in catechol-containing solutions, and the phenol is anodically oxidized. The product of this oxidation is highly reactive and undergoes reaction with chitosan chains adjacent to the anode. After reaction, the flexible chitosan film can be peeled from the wafer. Chemical and physical evidence support the conclusion that electrochemically initiated reactions crosslink chitosan. When gold is patterned onto the wafer, the electrochemical crosslinking reactions are spatially localized and impart anisotropic mechanical properties to the chitosan film. Further, deswelling of chitosan films can reversibly transduce environmental stimuli into contractile forces. Films patterned to have spatial variations in crosslinking respond to such environmental stimuli by undergoing reversible changes in shape. These results suggest the potential to enlist electrochemically initiated reaction cascades to engineer chitosan films for actuator functions.

1. Introduction

Biotechnology enables the creation of protein- and nucleic-acid-based materials to perform functions such as recognition, catalysis, signaling, and information storage/transfer. Interestingly, neither proteins nor nucleic acids are Nature's most abundant biopolymers. Polysaccharides and polymeric phenolics (e.g., lignins) are more abundant. We contend that the reaction cascades that generate phenolic materials are understudied but offer a potentially useful route to functional materials. In this work, we mimic poorly characterized phenol reaction cascades that are common in Nature with the goal of controllably altering the mechanical properties of a polysaccharide film.

In Nature, phenol reaction cascades are initiated by the enzymatic oxidation of phenols into reactive intermediates that undergo subsequent, uncatalyzed reactions. The initiating enzymes include tyrosinases, peroxidases, and laccases, and the reactive intermediates are typically quinones or free radicals. While the reaction cascades are difficult to study and sometimes controversial,[1–6] there is little doubt of the product's mechanical functions. For instance, lignification is initiated by the enzymatic oxidation of phenylpropanes and yields a complex 3D network that confers strength to trees. Sclerotization is initiated by the enzyme-catalyzed oxidization of low-molecular-weight phenols that appear to crosslink polymeric components of the insect's integument to yield hardened (i.e., quinone-tanned) "shells".[7–11] Curing of the mussel's adhesive protein is initiated by the enzymatic oxidation of some of its phenolic moieties (i.e., tyrosine or dihydroxyphenylalanine residues) to yield the crosslinked network needed for cohesive strength.[4,6,12] Over the years there have been several technological efforts to enlist these reactions to confer mechanical properties upon materials (e.g., to generate crosslinked adhesives,[13–16] fibers,[17] or gels[18,19]).

We contend that phenol reaction cascades could be more effectively exploited if their initiation could be controlled spatially and temporally. Nature controls cascade initiation by compartmentalization (the phenols and initiating enzymes are stored separately), or by the localized activation of inactive pro-enzymes. Compartmentalization is illustrated by the separate storage of polyphenol oxidase enzymes and phenolic reactants in plant tissue, and the requirement for tissue disruption for contact.[20–23] Pro-enzyme activation is illustrated by the in-

[*] Prof. G. F. Payne, Dr. L.-Q. Wu, Dr. C. Zhu
Center for Biosystems Research
University of Maryland Biotechnology Institute
5115 Plant Sciences Building, College Park, MD 20742 (USA)
E-mail: payne@umbi.umd.edu
Prof. G. F. Payne
Department of Chemical and Biochemical Engineering
University of Maryland, Baltimore County
1000 Hilltop Circle, Baltimore, MD 21250 (USA)
Dr. M. K. McDermott
Division of Chemistry and Materials Science
Office of Science and Engineering Laboratories
Food and Drug Administration
9200 Corporate Blvd., HFZ-150, Rockville, MD 20850 (USA)
Prof. R. Ghodssi
Department of Electrical and Computer Engineering
University of Maryland at College Park
College Park, MD 20742 (USA)
Prof. R. Ghodssi
The Institute for Systems Research
University of Maryland at College Park
College Park, MD 20742 (USA)

[**] Financial support was provided by the National Science Foundation (BES-0114790 and DMI-0321657).

nate immunity of insects where a phenoloxidase pro-enzyme appears to be activated upon pathogen invasion.[24–26] However, compartmentalization and pro-enzyme activation may not be the most convenient technological means to control the initiation of phenol reaction cascades. One technological approach for the control of phenol reactions is to couple enzyme-initiation with dip-pen nanolithography.[27–29]

We have employed a different technological approach to control initiation of the phenol reaction cascade. Specifically, we initiate this cascade electrochemically using micropatterned electrodes that allow control in space (based on the initial electrode patterning) and in time (based on when the electrodes are biased to initiate oxidation).[30] Also, electrochemical reactions can be initiated over relatively large surfaces in parallel operations (as compared to serial writing operations). The goals of this study are to enlist the phenol reaction cascade in order to controllably introduce crosslinks into a film of the aminopolysaccharide chitosan,[31] and to demonstrate that the mechanical properties of these films can be modified in predictable ways. We selected chitosan because it has nucleophilic primary amines at nearly every repeating sugar residue, and these amines are known to react with oxidized phenols.[32]

2. Results and Discussion

2.1. Chemical Evidence to Support Crosslinking

We performed two studies to examine whether electrochemically initiated reactions can crosslink chitosan. In the first study, we electrochemically oxidized catechol in the presence of films of both chitosan and a control polysaccharide (agar) that lacks such nucleophilic amines. Figure 1a shows that before reaction, neither the chitosan film nor the agar control absorbs above 300 nm. After reaction, the chitosan film was visually observed to be reddish-brown and Figure 1a shows its strong UV-vis absorbance. The absorption peak at 466 nm is consistent with the formation of Michael-type adducts between quinones and amines,[33,34] and quinones and chitosan.[35] While this UV-vis absorbance is consistent with a covalent grafting of the oxidized intermediates to chitosan, the observation that the reacted chitosan could not be dissolved under acidic conditions is consistent with covalent crosslinking. Figure 1a shows that agar's UV-vis absorbance is unchanged by the electrochemical reaction, suggesting this film does not react with oxidized catechol intermediates. Further, the "reacted" agar film could be dissolved upon heating. These results indicate that oxidized catechol can react with chitosan but not agar, and suggest that chitosan's amines participate in the reaction.

In a second study, we electrochemically oxidized catechol in the presence of glucosamine, the monomeric unit of chitosan, and analyzed the product solution using electrospray mass-spectrometry (ES-MS). The complexity of phenol reaction cascades is evidenced by a large number of product peaks observed in the ES-MS spectrum—Figure 1b shows a narrow region of this spectrum. The inset in Figure 1b shows two putative products that could be formed from the reaction of two glucosamine molecules with a single catechol. These putative products could be generated through intermediate Schiff-base linkages or Michael-type adducts,[35–37] and their expected $M+1$ (mass of protonated molecular ion) peaks are observed at m/z values of 433 and 449. The indication that electrochemically oxidized catechol is capable of reacting with two glucosamines suggests that these reactions are capable of crosslinking chitosan.

2.2. Analysis to Quantify the Reaction Chemistry

Quantitative information was obtained by performing electrochemically initiated reactions under defined conditions and measuring the "product" generated. Specifically, we patterned a wafer to have electrodes of different area (A) and we applied a constant current density (i) to each electrode so the total applied current (I) could be varied based on the electrode area. This wafer was coated with chitosan (thickness D), immersed in a solution containing catechol, and the electrode surface was biased to initiate reaction. Figure 2a illustrates that catechol must diffuse through the chitosan film to be oxidized at the anode, and the oxidized intermediate rapidly reacts with chitosan such that the thickness of the film's reacted zone (d_{rxnzone}) grows over time. After reaction, the film was washed extensively, peeled from the wafer, and the individual reacted regions were cut and washed with acetic acid (0.2 M) to dissolve away any unreacted chitosan. The acid-insoluble "product" was recovered, dried, and weighed, and Figure 2b shows a linear increase in mass of the acid-insoluble product (m_{product}) with current.

To provide a theoretical framework to analyze these experimental results, it is necessary to make assumptions about the electrochemical initiation reaction, and the structure of the resulting product. Assuming a two-electron anodic oxidation of

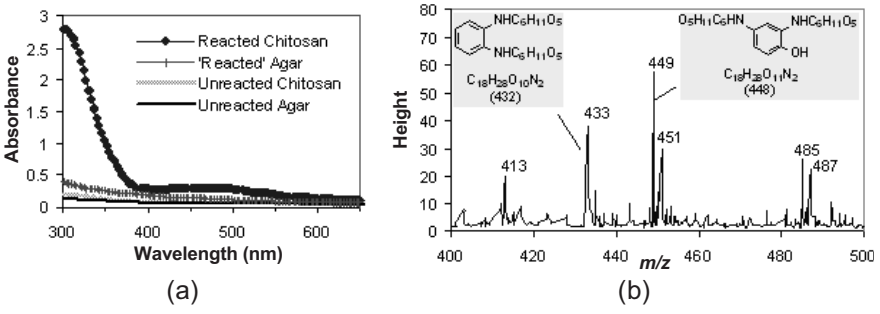

Figure 1. Chemical evidence that electrochemical reactions can crosslink chitosan. a) UV-vis spectra for agar and chitosan films before and after reaction with catechol (0.2 M) for 10 min at 0.4 mA cm^{-2}. b) Electrospray mass spectrum for product solution formed during electrochemical reaction of catechol (0.2 M) and glucosamine (0.4 M) for 10 min at 0.4 mA cm^{-2} (insets show structures and masses for putative crosslinks).

ADVANCED FUNCTIONAL MATERIALS

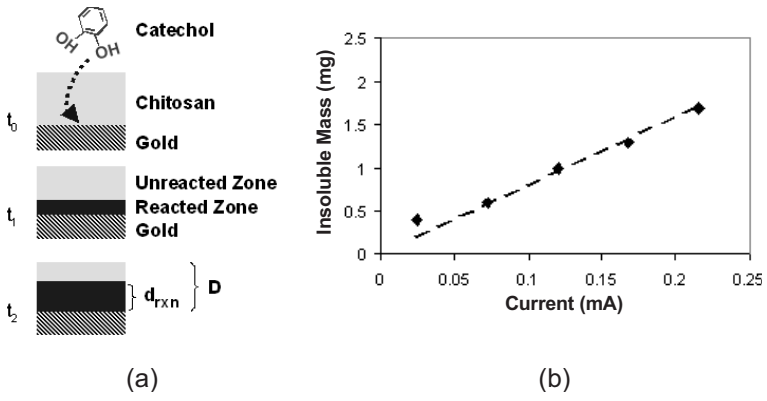

Figure 2. Quantification of electrochemically mediated chitosan reaction. a) Schematic showing catechol's diffusion through the chitosan film and oxidization at the anode, and reaction between the oxidized intermediate and chitosan. b) Mass of the acid-insoluble product generated as function of applied current. Electrochemical reactions of chitosan-coated wafers were performed for 20 min using catechol (0.02 M) and a current density of 0.2 mA cm^{-2}. The current was varied using a wafer that was fabricated to have five electrode surfaces of differing area but connected to the same lead.

catechol ($z = 2$), then the catechol reaction flux ($j_{catechol}$) can be related to the current density by

$$j_{catechol} = i/zF \tag{1}$$

where F is Faraday's constant.

Based on the ES-MS results, we assume each oxidized catechol crosslinks two glucosamine residues to form a "product" ($v_{product} = 1$ mol product/mol catechol) of molecular weight $MW_{product} \approx 440$ g mol^{-1}. For reactions performed at constant i for time t over an anode of area A, then the mass of product formed by this electrochemically initiated reaction should be

$$m_{product} = \left(v_{product}(MW_{product})\frac{t}{zF}\right)iA = \left(v_{product}(MW_{product})\frac{t}{zF}\right)I \tag{2}$$

Using assumed values and experimental conditions, Equation 2 predicts the slope of Figure 2b should be 2.7 mg mA^{-1}, which is within a factor of three of the experimentally observed value of 8.0 mg mA^{-1}. In light of the complexity of the reaction cascade, we believe this order-of-magnitude agreement between theory and experiment is remarkable. Importantly, this model assumes every glucosamine residue undergoes crosslinking, which suggests that the reacted chitosan films are highly crosslinked.

This quantitative analysis can be extended to estimate how fast the zone of reacted chitosan grows. The growth velocity for the reacted zone ($V_{rxnzone}$) can be estimated as

$$V_{rxnzone} = \frac{v_{chitosan}MW_{chitosan}}{x_{chitosan}\rho_{film}}j_{catechol} \tag{3}$$

where $v_{chitosan}$ is the stoichiometric ratio of glucosamine to catechol (assumed to be 2), $MW_{chitosan}$ is the molecular weight of the glucosamine repeating unit (160 g mol^{-1}), $x_{chitosan}$ is the weight fraction of chitosan in the wet film (measured to be 0.25 g chitosan/g film), and ρ_{film} is the density of the wet film (assumed to be 1 g cm^{-3}). Under conditions of constant i, the thickness of the reacted zone ($d_{rxnzone}$) at time t can be estimated from

$$d_{rxnzone} = V_{rxnzone}t = \left(\frac{v_{chitosan}MW_{chitosan}}{x_{chitosan}\rho_{film}}j_{catechol}\right)t \tag{4}$$

Using values for the experiment in Figure 2b, we estimate that during the 20 min reaction, 16 μm of the chitosan film underwent reaction. This compares with the initial film thickness of 45 μm.

2.3. Physical Evidence to Support Crosslinking

Crosslinking substantially alters the mechanical properties of polymeric networks,[38] and classical theories predict a linear dependence of the Young's modulus (E) on the crosslink density (μ). By invoking a commonly used set of assumptions for the network (e.g., four elastically active chain segments per crosslink), these theories predict[39]

$$E = 6\mu RT \tag{5}$$

Experimentally, we cast a 30 μm chitosan film onto a silicon wafer patterned with differing electrode areas, and set the electrochemical reaction conditions to completely react the film (i.e., $d_{rxnzone} \approx D = 30$ μm). After reaction, the films were carefully cut and the modified films were subjected to tensile testing. The stress–strain curves in Figure 3a show that compared to the unreacted chitosan control, the reacted chitosan films have a much larger slope (i.e., larger E). Also, Figure 3a shows that the slopes for all of the modified films are similar, which is expected since all films were modified to the same extent (i.e., the same $d_{rxnzone}$) despite having differing lateral dimensions. Figure 3b summarizes the experimentally determined values of E for these reacted chitosan films. Using an average value of E of 37 MPa for the reacted films, Equation 5 suggests a crosslink density for the reacted films of 2.5×10^3 mol m^{-3}. This is comparable to the estimated concentration of glucosamine residues (1.6×10^3 mol m^{-3}) for our wet films (25 % chitosan). This order-of-magnitude agreement further supports the conclusion that electrochemical reactions generate highly crosslinked films.

While the high value of E for the reacted chitosan film is consistent with a highly crosslinked network, it is interesting to note that E for the unreacted chitosan film is only a factor of five less. This suggests that the unreacted chitosan films also have a high crosslink density (although lower than that for the reacted films). For unreacted chitosan, the crosslinks are not permanent (i.e., the unreacted films dissolve in acid) and presumably result from interpolymer non-covalent associations.[40]

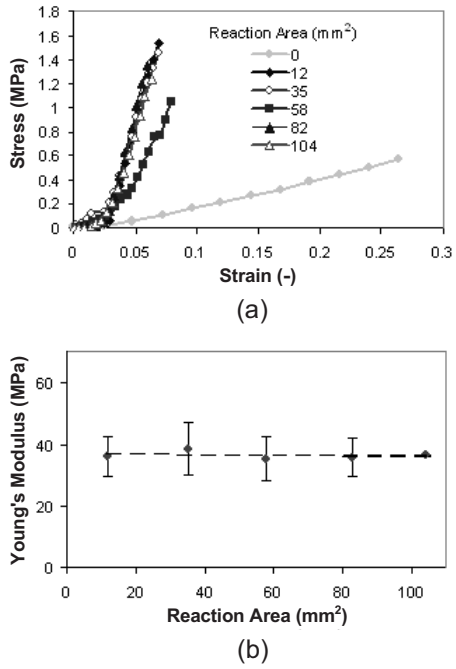

Figure 3. Physical evidence that electrochemical reactions crosslink chitosan. a) Comparison of stress–strain curves for 30 μm chitosan films reacted over differing lateral areas with an unreacted control (i.e., reaction area = 0 mm^2). b) Averaged Young's modulus (E) for reacted chitosan films as function of reaction area. All reactions were performed with catechol (0.2 M) for 20 min at 0.4 $mA\,cm^{-2}$. Note: the Young's moduli for the reacted films are expected to be independent of the reaction area since all films are reacted to the same extent (i.e., the same $d_{rxnzone}$).

2.4. Mechanical Properties of Films Depend on the Extent of Reaction

In principle, the ability to localize electrochemical crosslinking should enable the mechanical properties of chitosan films to be predictably altered. Specifically, Figure 4a illustrates that films can be prepared to any desired $d_{rxnzone}$ (less than the total film thickness D), while the modulus (E) for such partially reacted films should depend on the volume fractions (ϕ) and moduli of the reacted and unreacted regions. For the case of an applied load distributed in parallel between the reacted and unreacted regions, then mechanical models of composites (e.g., simple rules of mixing) suggest

$$E = \phi_{\text{unreacted}} E_{\text{unreacted}} + \phi_{\text{reacted}} E_{\text{reacted}} \quad (6)$$

Since $\phi_{\text{reacted}} + \phi_{\text{unreacted}} = 1$, Equation 6 simplifies to:

$$E = E_{\text{unreacted}} + (E_{\text{reacted}} - E_{\text{unreacted}})\phi_{\text{reacted}} \quad (7)$$

For simplicity, we assume that mass and volume fractions are equivalent, such that

$$\phi_{\text{reacted}} = d_{\text{rxnzone}}/D \quad (8)$$

Combining Equations 4 and 8

$$\phi_{\text{reacted}} = \frac{d_{\text{rxnzone}}}{D} = \frac{V_{\text{rxnzone}} t}{D} = \left(\frac{v_{\text{chitosan}} MW_{\text{chitosan}}}{x_{\text{chitosan}} \rho_{\text{film}} D} j_{\text{catechol}} \right) t \quad (9)$$

For conditions in which all bracketed terms in Equation 9 are constant, then Equations 7 and 9 predict the Young's modulus to increase linearly with reaction time.

To test this prediction, we cast a 30 μm chitosan film onto a wafer patterned with 1 mm electrodes and performed electrochemical reactions for varying times. The partially reacted 1 mm wide specimens were then analyzed by tensile testing. The stress–strain curves in Figure 4b show that as the extent of reaction increased, the specimens became stiffer (i.e., larger E) and more brittle (i.e., they failed at lower strains). Figure 4c shows that the observed modulus for the partially reacted chitosan specimens increased linearly with reaction time as predicted from Equations 7 and 9. The scatter observed in E for specimens that had been extensively reacted for 40 min is likely due to the difficulties encountered in handling these brittle specimens. Interestingly, we estimate that the chitosan specimens were completely reacted before 30 min, and thus speci-

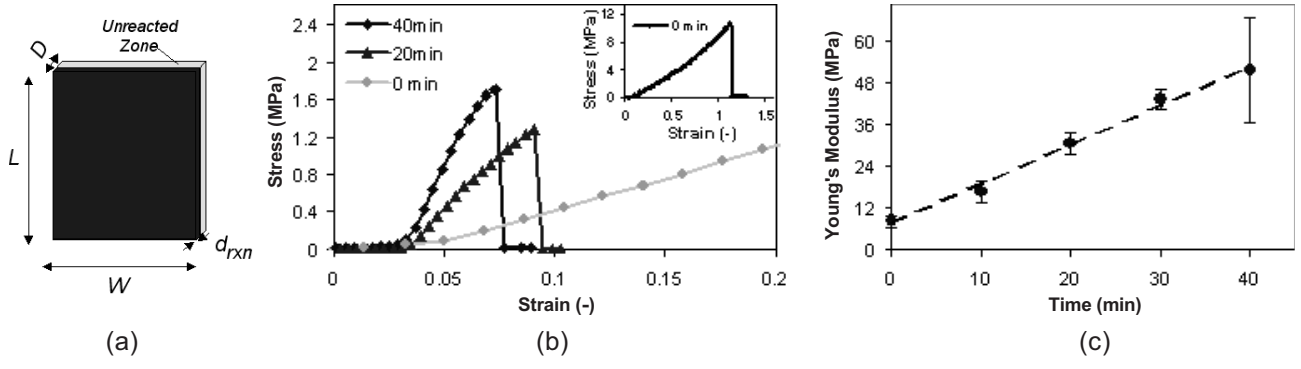

Figure 4. Mechanical properties of partially reacted chitosan films depend on extent of reaction. a) Schematic showing partially reacted chitosan films ($d_{rxnzone} < D$). b) Stress–strain curves for 30 μm chitosan films reacted for different times (inset shows expanded scale for the unreacted chitosan control). c) E of the chitosan films as function of reaction time. Equations 7 and 9 predict a linear relation between E and t. All reactions were performed with catechol (0.2 M) at 0.4 $mA\,cm^{-2}$.

mens modified for 40 min may have been qualitatively different (e.g., the specimens may become "overreacted" through additional chemistries).

2.5. Electrochemical Patterning Imparts Anisotropic Mechanical Properties

Figure 5a suggests that electrochemical crosslinking can be spatially controlled to generate patterned chitosan films, and that these films should offer spatially varying mechanical properties. To test this prediction, we fabricated a silicon wafer with 1 mm wide parallel gold electrodes spaced 1 mm apart. A 30 μm chitosan film was cast over this patterned wafer, the chitosan-coated wafer was electrochemically reacted with catechol, and the film was peeled from the wafer. A photograph of the patterned chitosan film is shown in Figure 5b and demonstrates that electrochemical reactions are spatially localized. These patterned films were tensile tested in both longitudinal (Lg) and transverse (Tr) directions, and the differences observed in Figure 5c demonstrate that these electrochemically patterned films have anisotropic mechanical properties. Figure 5c also shows the stress–strain curve for the unreacted chitosan control which shows no spatial variation in properties.

Quantitative predictions of the films' anisotropic properties can be obtained from mechanical models of composites. Based on our model estimates, the reaction conditions set in the experiment are sufficient to fully react the film in the patterned region (i.e., $d_{\mathrm{rxnzone}} \approx D$ in the patterned region). Thus, differences in ϕ_{reacted} and $\phi_{\mathrm{unreacted}}$ are due to differences in lateral patterning, and not to differences in the depth of the reaction zone as in Figure 4. For the pattern tested, ϕ_{reacted} and $\phi_{\mathrm{unreacted}}$ are 0.6 and 0.4, respectively. When stress is applied longitudinally, the reacted and unreacted regions are deformed in parallel and under this condition, Equation 6 is applicable.

$$E_{\mathrm{Lg}} = E_{\mathrm{unreacted}} + (E_{\mathrm{reacted}} - E_{\mathrm{unreacted}})\phi_{\mathrm{reacted}} \quad (10)$$

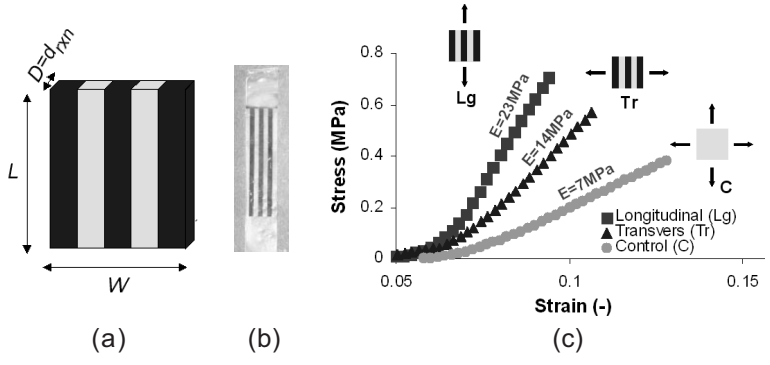

Figure 5. Electrochemical patterning with catechol confers anisotropic mechanical properties upon chitosan films. a) Schematic of the electrochemically patterned chitosan film. b) Photograph of the patterned film. c) Stress–strain curves for patterned films in Tr and Lg directions, and for an unreacted chitosan control. All reactions were performed with catechol (0.2 M) for 20 min at 0.4 mA cm^{-2}. The pattern consisted of three 1 mm wide reacted regions separated by two 1 mm wide unreacted regions.

Using average values of $E_{\mathrm{reacted}} \approx 37$ MPa (Fig. 3b) and $E_{\mathrm{unreacted}} \approx 7$ MPa (Fig. 5c), Equation 10 predicts an E_{Lg} of 25 MPa. Figure 5c and Table 1 indicate that this expected E_{Lg} is similar to that observed experimentally.

When the patterned film is tensile tested in the transverse direction, the unreacted and reacted regions are loaded in series, and composite models predict

$$E_{Tr} = \frac{1}{\left(\frac{\phi_{\mathrm{unreacted}}}{E_{\mathrm{unreacted}}} + \frac{\phi_{\mathrm{reacted}}}{E_{\mathrm{reacted}}}\right)} \quad (11)$$

Using the values from above, Equation 11 predicts an E_{Tr} of 14 MPa, which is again in good agreement with the experimentally measured values of Figure 5c and Table 1. These results demonstrate that electrochemical patterning imparts predictable, spatially varying mechanical properties to the chitosan film.

Table 1. Average value of Young's modulus and strain to failure for unreacted chitosan films, and patterned chitosan films strained in transverse (Tr) and longitudinal (Lg) directions. Films were patterned as illustrated in Figure 5.

Chitosan film		Young's modulus [MPa]	Strain to failure
Unreacted		6 ± 4	2.2 ± 0.1
Patterned	Lg	21 ± 3	0.10 ± 0.03
	Tr	14 ± 4	0.16 ± 0.06

2.6. Electrochemical Patterning to Alter Chemomechanical Transduction

Crosslinked polymer networks reversibly swell and deswell in response to environmental stimuli and thus can transduce chemical stimuli into mechanical forces. The ability to generate chitosan films with spatially varying crosslink densities suggests that patterned films may offer unique chemomechanical transduction properties. To examine this potential, chitosan films were transferred between water and ethanol—conditions that lead to reversible swelling and deswelling of the chitosan network.

In our initial study, we compared the contractile forces generated by transferring patterned and unpatterned films from water to ethanol. The patterned film was created by casting a 30 μm chitosan film onto a wafer fabricated with a series of parallel 100 μm wide gold lines spaced 100 μm apart. Electrochemical reaction conditions were set to generate films that were both laterally patterned and partially reacted (we estimate $d_{\mathrm{rxnzone}}/D \approx 0.75$ for our experimental conditions) as illustrated in Scheme 1a. After reaction, the patterned film was peeled from the wafer and Scheme 1b shows that this specimen was loaded onto a tensile-testing instrument in a longitudinal direction. The specimen was prestretched to a small strain, and then re-adjusted to a strain that cor-

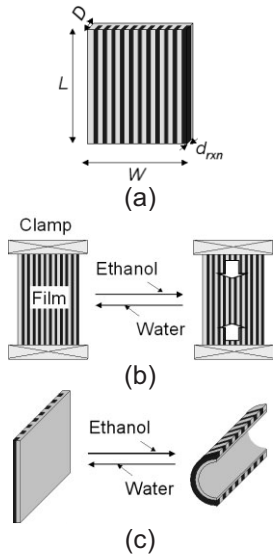

Scheme 1. Experimental approaches to study chemomechanical transduction. a) Films were patterned and partially reacted ($d_{rxnzone} < D$). b) Approach to study stimuli-responsive contractile forces. c) Approach to study stimuli-responsive shape changes.

responded to no stress. We then maintained a constant strain, exchanged the water in the bath for ethanol, and monitored the change in force exerted by the specimen.

Figure 6 shows that when the patterned chitosan film was subjected to the ethanol exchange step the film's deswelling exerted a contractile force of 0.23 N. This contractile force is eliminated when the film is re-immersed in water. Figure 6 shows these results are reproducible when the film is repeatedly subjected to solvent exchange. Additionally, this result is reproducible when separate films are subjected to the same treatment. Specifically, we observed a contractile force of

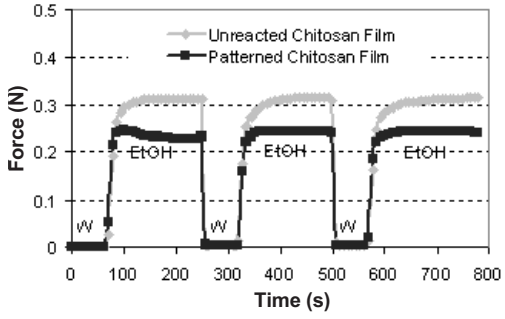

Figure 6. Patterned and partially reacted chitosan films have altered chemomechanical transduction properties. Electrochemical patterning of a 30 μm chitosan film was performed with catechol (0.2 M) for 15 min at 0.4 mA cm^{-2} to achieve $d_{rxnzone}/D \approx 0.75$. The patterned chitosan film used for testing had 25 100 μm wide reacted lines each separated by 100 μm unreacted spaces, and a 0.75 mm unreacted border on each side. These films were loaded onto a tensile testing instrument as illustrated in Scheme 1b and set to an unstressed condition with water (W). Exchange of the water with ethanol (EtOH) resulted in a contractile force—presumably due to deswelling of the network. Re-exchange from ethanol to water eliminates this contractile force—presumably due to re-swelling of the chitosan network. Patterning results in a quantitative difference in the ontractile force exerted by the film upon transfer into ethanol.

0.23 ± 0.02 N for the transfer from water to ethanol of six replicate patterned films. Figure 6 also shows that the unreacted chitosan control film behaves qualitatively similar to the patterned film. However, the contractile force exerted by the unreacted chitosan upon transfer to ethanol is 30 % larger (0.30 ± 0.01 N for eight replicate films). This larger contractile force for the unreacted film is presumably due to its lower crosslink density and greater ability to undergo volume changes upon swelling and deswelling. These results demonstrate that electrochemical crosslinking quantitatively alters the film's chemomechanical transduction of environmental stimuli.

Scheme 1c suggests that it may be possible to use these quantitative differences to transduce environmental stimuli into controlled shape changes for patterned films. To test this possibility, we prepared three films, an unreacted control, and two films patterned with 100 μm parallel lines separated by 100 μm spaces as described in Figure 6. As illustrated in the schemes in Figure 7, one end of each film was anchored by sandwiching it between two glass slides. Figure 7a shows that the unpatterned control film shrinks somewhat upon transferring it from water

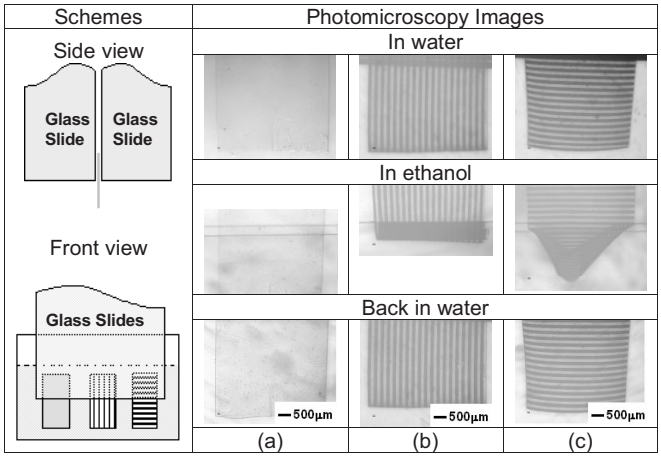

Figure 7. Chemomechanical transduction of patterned films to convert environmental stimuli into shape changes. Schemes show an unreacted film, and two patterned films that are sandwiched between glass slides and transferred between solvents. a) The unreacted chitosan control film changes size but not shape upon transfer from water to ethanol and back to water. b) A patterned film with the lines perpendicular to the edge of the glass rolls up to the edge of the glass slides in ethanol. c) A patterned film with lines parallel to the edge of the glass has a tendency to roll up in ethanol, but this tendency is constrained by anchoring between the glass slides.

to ethanol, and then re-swells upon returning it to water. While film shrinkage is difficult to visualize in this image of a transparent film, the absence of specific shape changes is apparent in Figure 7a. Figure 7b shows that when the patterned film is sandwiched between the glass slides with its lines normal to the edge of the glass, then transfer to ethanol results in a rolling up of the film. Figure 7c shows that when the patterned film is aligned with its lines parallel to the edge of the glass, then the tendency for the film to roll up is impeded by its anchoring between the two glass surfaces. These images demonstrate that

patterning confers on the chitosan film a tendency to change shape (i.e., to roll up) along a preferred axis. In both cases, the patterned films returned to their original shape when they were transferred from ethanol back into water, and these shape changes were repeatable.

A final observation is illustrated in Scheme 1c. Specifically, we visually observed the patterned and partially reacted films of Figure 7 roll toward their unreacted face. This orientation is expected since we believe the unreacted face will be able to deswell more than the highly crosslinked reacted face.

3. Conclusions

Advances over the last few decades have allowed proteins, nucleic acids, and, to a lesser extent, polysaccharides[41,42] to be precisely constructed to perform complex functions (e.g., recognition, catalytic, and informational). Compared to these biopolymers, biological materials derived from phenols are largely unstudied. The fact that phenol-based materials are ubiquitous in Nature suggests that an ability to control the underlying phenol reaction cascades may provide new opportunities for conferring diverse functionalities for technological applications.

We mimicked natural phenol reactions using electrochemical oxidation to initiate a cascade that chemically and mechanically alters a flexible film of the polysaccharide chitosan. Chemical and physical evidence indicates that anodic catechol oxidation can crosslink these films. Because electrochemical oxidation can be performed at patterned anodes, crosslinking can be spatially controlled to impart predictable mechanical properties to the films. Experimental results agree with quantitative predictions that increases in the extent of reaction will yield systematic increases in the Young's modulus, while patterning will confer anisotropic mechanical properties. Qualitative expectations that crosslinking will alter the film's responsiveness to environmental stimuli are consistent with contractile force measurements, and with shape changes observed for patterned films upon transfer between swelling and deswelling solvents. Together, the ability to localize phenol reaction cascades[30] and the observation that the chemomechanical properties of these films are altered by these reactions suggests the potential to engineer chitosan films to perform finely tuned actuator functions.[43–47]

4. Experimental

Chitosan was reported by the supplier (Sigma–Aldrich) to have a degree of acetylation of 15 % and was dissolved in dilute HCl solution as described elsewhere [48]. Gold was patterned onto silicon wafers using standard photolithographic methods [48] and the wafers were cut into appropriate sizes for each experiment (we use the term "wafer" to refer to the cut pieces used in individual experiments). UV-vis spectra were obtained using a Spectronic Genesys II. Electrospray mass spectra were collected at the University of Maryland's Mass Spectrometry facility (http://www.chem.umd.edu/facility/masspect.php).

Chitosan was coated onto patterned wafers by dip-casting using a 2.5 wt % chitosan solution. The chitosan-coated wafers were dried at 55 °C for 40 min, neutralized in 1 M NaOH for 10 min, and then rinsed extensively with distilled water. For electrochemical pattern transfer, the chitosan-coated wafer was immersed in a 20 mM phosphate buffer (pH 6.5) containing the phenol catechol. Pattern transfer was initiated by biasing the patterned gold surface (i.e., the anode) using a DC power supply (Agilent 6614C) to achieve a constant current density. An unpatterned, gold-coated wafer served as the cathode for this electrochemical reaction. After the reaction, the wafer was disconnected from the power supply, removed from the catechol solution, and rinsed with distilled water.

Stress–strain curves were generated using a dynamic mechanical thermal analyzer (DMTA; Rheometric Scientific). All tensile tests were performed with the samples immersed in a water bath at 37 °C. The DMTA was also used to measure the force generated when a film was transferred between water and ethanol—these measurements were performed using solvents pre-equilibrated to room temperature. In these studies, each film was first subjected to a small strain while immersed in water to identify the appropriate spacing between the grips. The spacing was then adjusted to a position in which the films were unstressed. This spacing was maintained constant, and the solvent was exchanged while the force was being measured.

Photomicroscopy images of the unpatterned and patterned chitosan films were obtained using an optical microscope (Model FS70, Mitutoyo Corp.) with a digital camera (Nikon DXM 1200).

Received: November 9, 2005
Final version: February 3, 2006
Published online: August 21, 2006

[1] K. B. Stark, J. M. Gallas, G. W. Zajac, M. Eisner, J. T. Golab, *J. Phys. Chem. B* **2003**, *107*, 3061.
[2] A. M. Rouhi, *Chem. Eng. News* **2001**, *April 2*, 52.
[3] B. J. Powell, T. Baruah, N. Bernstein, K. Brake, R. H. McKenzie, P. Meredith, M. R. Pederson, *J. Chem. Phys.* **2004**, *120*, 8608.
[4] L. A. Burzio, J. H. Waite, *Biochemistry* **2000**, *39*, 11 147.
[5] J. Schaefer, K. J. Kramer, J. R. Garbow, G. S. Jacob, E. O. Stejskal, T. L. Hopkins, R. D. Speirs, *Science* **1987**, *235*, 1200.
[6] L. M. McDowell, L. A. Burzio, J. H. Waite, J. Schaefer, *J. Biol. Chem.* **1999**, *274*, 20 293.
[7] K. Kramer, M. Kanost, T. Hopkins, H. Jiang, Y. Zhu, R. Xu, J. Kerwin, F. Turecek, *Tetrahedron* **2001**, *57*, 385.
[8] M. R. Chase, K. Raina, J. Bruno, M. Sugumaran, *Insect Biochem. Mol. Biol.* **2000**, *30*, 953.
[9] M. Sugumaran, *Adv. Insect Physiol.* **1988**, *21*, 179.
[10] S. O. Andersen, M. G. Peter, P. Roepstorff, *Comp. Biochem. Physiol. B: Biochem. Mol. Biol.* **1996**, *113*, 689.
[11] M. G. Peter, *Angew. Chem. Int. Ed. Engl.* **1989**, *28*, 555.
[12] J. H. Waite, *Int. J. Biol. Macromol.* **1990**, *12*, 139.
[13] J. L. Dalsin, B. H. Hu, B. P. Lee, P. B. Messersmith, *J. Am. Chem. Soc.* **2003**, *125*, 4253.
[14] T. J. Deming, *Curr. Opin. Chem. Biol.* **1999**, *3*, 100.
[15] K. Yamada, T. Chen, G. Kumar, O. Vesnovsky, L. D. Topoleski, G. F. Payne, *Biomacromolecules* **2000**, *1*, 252.
[16] M. Yu, T. J. Deming, *Macromolecules* **1998**, *31*, 4739.
[17] Y. Kuboe, H. Tonegawa, K. Ohkawa, H. Yamamoto, *Biomacromolecules* **2004**, *5*, 348.
[18] B. P. Lee, J. L. Dalsin, P. B. Messersmith, *Biomacromolecules* **2002**, *3*, 1038.
[19] G. Kumar, J. F. Bristow, P. J. Smith, G. F. Payne, *Polymer* **2000**, *41*, 2157.
[20] A. M. Mayer, *Phytochemistry* **1987**, *26*, 11.
[21] K. Vaughn, A. Lax, S. Duke, *Physiol. Plant.* **1988**, *72*, 659.
[22] G. W. Felton, K. Donato, R. J. Del Vecchio, S. S. Duffey, *J. Chem. Ecol.* **1989**, *15*, 2667.
[23] J. C. Steffens, E. Harel, M. D. Hunt, *Recent Adv. Phytochem.* **1994**, *28*, 275.
[24] A. J. Nappi, B. M. Christensen, *Insect Biochem. Mol. Biol.* **2005**, *35*, 443.

[25] B. M. Christensen, J. Li, C. C. Chen, A. J. Nappi, *Trends Parasitol.* **2005**, *21*, 192.
[26] X. Zhao, M. Ferdig, B. Christensen, *Dev. Comp. Immunol.* **1995**, *19*, 205.
[27] P. Xu, D. L. Kaplan, *Adv. Mater.* **2004**, *16*, 628.
[28] P. Xu, D. L. Kaplan, *J. Macromol. Sci., Part A: Pure Appl. Chem.* **2004**, *A41*, 1437.
[29] P. Xu, H. Uyama, J. E. Whitten, S. Kobayashi, D. L. Kaplan, *J. Am. Chem. Soc.* **2005**, *127*, 11 745.
[30] L. Q. Wu, R. Ghodssi, Y. A. Elabd, G. F. Payne, *Adv. Funct. Mater.* **2005**, *15*, 189.
[31] H. Yi, L. Q. Wu, W. E. Bentley, R. Ghodssi, G. W. Rubloff, J. N. Culver, G. F. Payne, *Biomacromolecules* **2005**, *6*, 2881.
[32] R. A. A. Muzzarelli, G. Littarrua, C. Muzzarelli, G. Tosi, *Carbohydr. Polym.* **2003**, *53*, 109.
[33] M. Garciamoreno, J. N. Rodriguezlopez, F. Martinezortiz, J. Tudela, R. Varon, F. Garciacanovas, *Arch. Biochem. Biophys.* **1991**, *288*, 427.
[34] L. H. Shao, G. Kumar, J. L. Lenhart, P. J. Smith, G. F. Payne, *Enzyme Microb. Technol.* **1999**, *25*, 660.
[35] L. Q. Wu, H. D. Embree, B. M. Balgley, P. J. Smith, G. F. Payne, *Environ. Sci. Technol.* **2002**, *36*, 3446.
[36] C. M. Aberg, T. H. Chen, A. Olumide, S. R. Raghavan, G. F. Payne, *J. Agricult. Food Chem.* **2004**, *52*, 788.
[37] J. L. Kerwin, D. L. Whitney, A. Sheikh, *Insect Biochem. Mol. Biol.* **1999**, *29*, 599.
[38] K. S. Anseth, C. N. Bowman, L. Brannon-Peppas, *Biomaterials* **1996**, *17*, 1647.
[39] L. Sperling, *Introduction to Physical Polymer Science*, Wiley, New York **2001**, p. 424.
[40] A. Montembault, C. Viton, A. Domard, *Biomacromolecules* **2005**, *6*, 653.
[41] J. M. Whitelock, R. V. Iozzo, *Chem. Rev.* **2005**, *105*, 2745.
[42] R. Raman, V. Sasisekharan, R. Sasisekharan, *Chem. Biol.* **2005**, *12*, 267.
[43] D. J. Beebe, J. S. Moore, J. M. Bauer, Q. Yu, R. H. Liu, C. Devadoss, B.-H. Jo, *Nature* **2000**, *404*, 588.
[44] T. F. Otero, J. M. Sansinena, *Adv. Mater.* **1998**, *10*, 491.
[45] X. Chen, W. J. Li, W. Zhong, Y. H. Lu, T. Y. Yu, *J. Appl. Polym. Sci.* **1997**, *65*, 2257.
[46] T. Tanaka, *Sci. Am.* **1981**, *244*, 124.
[47] L. F. Gudeman, N. A. Peppas, *J. Appl. Polym. Sci.* **1995**, *55*, 919.
[48] L.-Q. Wu, H. Yi, S. Li, G. W. Rubloff, W. E. Bentley, R. Ghodssi, G. F. Payne, *Langmuir* **2003**, *19*, 519.